

Reinforcement Design in Wind Turbine Foundations Using Three-Dimensional Solid Finite Element Modeling

ASSIS A. R. M. G.[1], ZAMPIERI L. Q.[2], BLASI H. R.[3]

[1]*Dept. of Structural and Geotechnical Engineering, Araxá Engenharia*
R. Demétrio Ribeiro, 57, 88020-710, SC, Brazil
alysson.assis@araxaeng.com.br, alyssondeassis@gmail.com
[2]*Dept. of Structural and Geotechnical Engineering, Araxá Engenharia*
R. Demétrio Ribeiro, 57, 88020-710, SC, Brazil
lucas.zampieri@araxaeng.com.br
[3]*Dept. of Structural Engineering, Statkraft*
Rod. José Carlos Daux, 5500, 88032-005, SC, Brazil
hhenriquebr@hotmail.com

Abstract. Wind turbines have played an increasingly important role in the global energy mix, acting as key players in the transition toward sustainable energy sources. Within the structural system that makes up these machines, the foundations occupy a critical position, guaranteeing stability and safety under the high dynamic and static loads imposed on them. Proper sizing of these foundations—especially their reinforced-concrete components—is essential for ensuring long-term structural performance and installation longevity. In Brazil, structural designs of wind-turbine foundations are typically verified using shell finite-element models. Although computationally efficient, such idealizations may fail to capture the complex three-dimensional stress distribution, particularly in regions with geometric discontinuities and at the interfaces between structural components. Given that foundation blocks usually feature massive geometries with irregular volumes and significant soil interaction, relying on shell models can lead to excessive simplifications that compromise the accuracy of reinforcement calculations. This article presents a reinforcement-design procedure based on three-dimensional models employing solid finite elements. The proposed approaches seeks to overcome the limitations inherent in shell idealizations, enabling a more accurate representation of internal stress states and yielding designs that are more robust and better aligned with real-world behavior. The paper discusses criteria for stress extraction and conversion into reinforcement, along with practical aspects of implementation and validation of the procedure.

Keywords: Wind turbines foundations, Structural design, FEM, Solid finite elements.

1 Introduction

Wind turbines have become increasingly relevant in the global energy matrix, playing a key role in the transition to sustainable energy sources. Within the structural system that supports these machines, foundations occupy a critical position, ensuring stability and safety under the significant static and dynamic loads to which they are subjected. The proper design of these foundations—particularly their reinforced concrete components—is essential to guarantee long-term structural performance and installation durability.

In Brazil, the structural analysis of wind turbine foundations is commonly performed using finite element models composed of shell elements. Although computationally efficient, such idealizations often fail to capture the full three-dimensional distribution of internal stresses, especially in regions with geometric discontinuities or at interfaces between structural components. This limitation may compromise the accuracy of reinforcement calculations, since foundation blocks typically exhibit massive geometries, irregular volumes, and significant soil-structure interaction. As stated by Stathopoulos & Baniotopoulos (2007), a complex stress state develops in the pedestal and the skirt of the foundation, resulting from the load combinations transferred from the tower to the foundation and from the pretensioned anchor bolts.[1]. According to Chen et al. [2], current structural design practice still relies predominantly on beam and shell elements, while the use of three-dimensional solid elements remains limited. This condition is partly due to the complexity involved in handling the large amount of output data

and, more importantly, the lack of well-established methods for reinforcement design based on three-dimensional stress fields.

International standards, such as those issued by the IEC [3], recognize the importance of solid finite elements in cases where the assumption of plane sections remaining plane is no longer valid — that is, when through-thickness strain distributions become nonlinear. Solid finite elements are also particularly suitable for capturing complex inelastic responses in concrete, such as cracking, reinforcement yielding, steel-concrete bond slip, and stiffness degradation due to crack propagation. For such analyses, reinforcement can be modeled using embedded truss bars, smeared reinforcement, or through automatic embedding capabilities available in simulation software. Proper representation of bond-slip behavior and interface separation may require the use of specialized interface elements. Additionally, for regions exhibiting geometric or load discontinuities—referred to as discontinuity regions —the use of strut-and-tie models or stress fields satisfying equilibrium conditions is recommended. These can be calibrated through simulations using solid finite elements [3].

In this study, the internal forces obtained through the numerical integration of results from solid finite elements are compared with those derived from shell-based models.

Subsequently, a reinforcement design procedure was adopted, based on formulations initially developed by Smirnov [4], Kamezawa [5] and Marti et al. [6], as cited by Chen et al [2]. In Brazil, these concepts have been incorporated into the Reinforced Solid Method (RSM), proposed by Chen, Bittencourt, and Della Bella (2023) [2], with the aim of enabling the practical application of solid finite element models [7, 8].

Finally, the reinforcement demand for a representative section is evaluated using the RSM and compared with the results obtained through principal equilibrium analysis under the Ultimate Limit State (ULS) [9].

2 Integration for obtaining internal forces.

The stress integration in the implemented post-processing routine is carried out according to the equations below, following the usual sign convention of Plate Theory to obtain the bending moment (M), axial force (N), and shear force (V). The integration limits correspond to the height of the member. Numerical integration is performed by calculating the area of the trapezoid formed by the stress difference at each node of the element along its height. [1]

$$\mathbf{N} = \begin{Bmatrix} N_x \\ N_y \\ N_{xy} \end{Bmatrix} = \int_{-h/2}^{h/2} \begin{Bmatrix} \sigma_x \\ \sigma_y \\ \tau_{xy} \end{Bmatrix} dz \tag{3}$$

$$\mathbf{M} = \begin{Bmatrix} M_x \\ M_y \\ M_{xy} \end{Bmatrix} = \int_{-h/2}^{h/2} \begin{Bmatrix} \sigma_x \\ \sigma_y \\ \tau_{xy} \end{Bmatrix} z\, dz \tag{4}$$

$$\mathbf{V} = \begin{Bmatrix} V_x \\ V_y \end{Bmatrix} = \int_{-h/2}^{h/2} \begin{Bmatrix} \tau_{xz} \\ \tau_{yz} \end{Bmatrix} dz \tag{5}$$

3 The Reinforced Solid Method (RSM)

Limit analysis provides the theoretical framework for the design of structures at the Ultimate Limit State (ULS), by establishing the conditions under which equilibrium is satisfied with materials exhibiting plastic behavior or yielding. According to the lower-bound theorem, any statically admissible stress field that does not exceed the material's strength will result in a load not greater than the actual collapse load of the structure. This approach

enables the formulation of design criteria based on actual stress states, provided that both equilibrium and local strength capacities are respected.

The Reinforced Solid Method (RSM), extends this rationale to the context of three-dimensional solid finite elements, enabling the direct design of reinforcement based on stress fields extracted from solid elements. The methodology is grounded in the principle that, for a structural model to be admissible in the ULS, the internal forces obtained from numerical analysis must be in equilibrium with the local strength of the concrete and reinforcement, in accordance with the assumptions of limit analysis.

The equation presents the decomposition of the total applied stress tensor $\mathbf{S}$ in a cracked concrete element with smeared reinforcement into two components: the concrete stress tensor $\mathbf{S}_c$ and the reinforcement stress tensor S_s. The model assumes that the reinforcement crosses the crack plane in the x, y and z directions and that the crack face itself does not transfer stress (neither normal nor shear). The concrete iss responsible for carrying the difference betweeen the total and reinforcement normal stresses, as well as all shear components. Meanwhile, the reinforcment resists only the equivalent normal stresses f_{tz}, f_{ty} and f_{tz}.

$$\mathbf{S} = \mathbf{S}_c + \mathbf{S}_s = \begin{bmatrix} \sigma_x - f_{tx} & \tau_{xy} & \tau_{xz} \\ \tau_{yx} & \sigma_y - f_{ty} & \tau_{yz} \\ \tau_{zx} & \tau_{zy} & \sigma_z - f_{tz} \end{bmatrix} + \begin{bmatrix} f_{tx} & 0 & 0 \\ 0 & f_{ty} & 0 \\ 0 & 0 & f_{tz} \end{bmatrix} \tag{1}$$

Concrete must resist both the difference between the applied normal stresses and the reinforcement normal stresses ($\sigma_{ci} = \sigma_i - f_{ti}$), and all three shear stress components ($\tau_{xy}, \tau_{xz}, \tau_{yz}$). Reinforcement, on the other hand, must carry only the equivalent reinforcement stresses f_{tx}, f_{ty}, f_{tz}, which represent the reinforcement forces per unit area of concrete. It is assumed that reinforcing steel does not carry shear stress. [2]

Out of the eight possible sign combinations of the three shear stress components, it is sufficient to consider only two representative cases for the calculation of the reinforcement: either all shear stresses are positive, or all are negative (which also covers the scenario where two components are positive and one is negative). This classification forms the basis for the subsequent formulation. For the complete derivation, the reader is referred to the work of Nielsen and Hoang. [2] [8]

Concrete stresses are required to satisfy:

$$\sigma_{III} \leq \nu f_{cd} \tag{2}$$

where f_{cd} is the design compression strength of concrete, and ν is the efficiency factor introduced to account for both, confinement effects and micro-cracking in the concrete paste due to shrinkaage. For more details about concrete check the reader is referred to the work of Chen et al. [2]

Table 1. RSM Design equations [2]

Reinf	Cases	f_{tx}	f_{ty}	f_{tz}	Condition
--‖--	1a +++	$\sigma_x + (\tau_{xy} + \tau_{xz})$	$\sigma_y + (\tau_{yx} + \tau_{yz})$	$\sigma_z + (\tau_{xz} + \tau_{yz})$	$f_{tx}, f_{ty}, f_{tz} > 0$
--‖--	2a ++-	$\sigma_x + (\tau_{xy} + \tau_{xz})$	$\sigma_y + (\tau_{xy} + \tau_{yz})$	$\sigma_z + (\tau_{xz} + \tau_{yz})$	$f_{tx}, f_{ty}, f_{tz} > 0$ $\tau_{xy}\tau_{xz} + \tau_{xz}\tau_{yz} + \tau_{xy}\tau_{yz} > 0$
--‖--	2b ++-	$\sigma_x - \frac{\tau_{xy}\tau_{xz}}{\tau_{yz}}$	$\sigma_y - \frac{\tau_{xy}\tau_{yz}}{\tau_{xz}}$	$\sigma_z - \frac{\tau_{xz}\tau_{yz}}{\tau_{xy}}$	$f_{tx}, f_{ty}, f_{tz} > 0$ $\tau_{xy}\tau_{xz} + \tau_{xz}\tau_{yz} + \tau_{xy}\tau_{yz} < 0$
-- --	1b/2	$\sigma_x + \tau_{xy} - \tau_{xz}\frac{\tau_{xz} + \tau_{yz}}{\sigma_z}$	$\sigma_y + \tau_{xy} - \tau_{yz}\frac{\tau_{xz} + \tau_{yz}}{\sigma_z}$	0	$f_{tz} < 0$ $f_{tx}, f_{ty} > 0$
--‖	1b/2	$\sigma_x + \tau_{xy} - \tau_{xz}\frac{\tau_{xz} + \tau_{yz}}{\sigma_y}$	0	$\sigma_z + \tau_{xz} - \tau_{yz}\frac{\tau_{xy} + \tau_{yz}}{\sigma_y}$	$f_{ty} < 0$ $f_{tx}, f_{tz} > 0$
‖--	1b/2	$0\sigma_x + \tau_{yz} - \tau_{xy}\frac{\tau_{xy} + \tau_{xz}}{\sigma_x}$	$\sigma_z + \tau_{yz} - \tau_{xz}\frac{\tau_{xy} + \tau_{xz}}{\sigma_x}$	$f_{tx} < 0$	 $f_{ty}, f_{tz} > 0$
--,	1c/2	$\sigma_x + \frac{2\tau_{xy}\tau_{xz}\tau_{yz} - \sigma_y\tau_{xz}^2 - \sigma_z\tau_{xy}^2}{\sigma_y\sigma_z - \tau_{yz}^2}$	0	0	$f_{ty}, f_{tz} < 0$ $f_{tx} > 0$
,--	1c/2	0	$\sigma_y + \frac{2\tau_{xy}\tau_{xz}\tau_{yz} - \sigma_x\tau_{yz}^2 - \sigma_z\tau_{xy}^2}{\sigma_x\sigma_z - \tau_{xz}^2}$	0	$f_{tx}, f_{tz} < 0$ $f_{ty} > 0$
‖	1c/2	0	0	$\sigma_z + \frac{2\tau_{xy}\tau_{xz}\tau_{yz} - \sigma_x\tau_{yz}^2 - \sigma_y\tau_{xz}^2}{\sigma_x\sigma_y - \tau_{xy}^2}$	$f_{tx}, f_{ty} < 0$ $f_{tz} > 0$
	1d/2	0	0	0	$\sigma_x\sigma_y\sigma_z + 2\tau_{xy}\tau_{xz}\tau_{yz}$ $-\sigma x\tau_{yz}^2 - \sigma_y\tau_{xz}^2$ $\sigma_z\tau_{xy}^2 < 0$

Notes:

1. Sign convention: positive normal stress for tension.
2. Case 1: (sign of τ_{xy}, sign of τ_{xz}, sign of τ_{yz}) = (+++), (+–), (–+), (-+-), ⇒ consider $+|\tau_{xy}|$, $+|\tau_{xz}|$, and $+|\tau_{yz}|$
3. Case 2: (sign of τ_{xy}, sign of τ_{xz}, sign of τ_{yz}) = (++-, +-+, -++, —)
   ⇒ If $|\tau_{yz}|$ is the smallest absolute shear stress: consider $+|\tau_{xy}|$, $+|\tau_{xz}|$, $-|\tau_{yz}|$.
   ⇒ If $|\tau_{xy}|$ is the smallest absolute shear stress: x–y, y–z, z–x axes. Consider $+|\tau_{xy}|$, $+|\tau_{xz}|$, and $-|\tau_{yz}|$. Calculate reinf. and retrieve original axes.
   ⇒ If $|\tau_{xz}|$ is the smallest absolute shear stress: x–z, y–x, z–y axes. Consider $+|\tau_{xy}|$, $+|\tau_{xz}|$, and $-|\tau_{yz}|$. Calculate reinf. and retrieve original axes.
4. Concrete stresses (all cases): $\sigma_{cx} = \sigma_x - f_{tx}$, $\sigma_{cy} = \sigma_y - f_{ty}$, $\sigma_{cz} = \sigma_z - f_{tz}$.
5. Reinforcement: $\rho_{sx} = f_{tx}/f_y$, $\rho_{sy} = f_{ty}/f_y$, $\rho_{sz} = f_{tz}/f_y$; and $\alpha_s = \rho_s.A_c$.

4 Principal Equilibrium

The principal equilibrium is determined by the two resistances of the cross section: the axial resistance of the section, N_{Rd}, and the bending resistance about the t-axis, M_{Rdt}. Since these resistances mutually influence each other, this interaction must be taken into account. For this purpose, a failure surface is defined to establish a safe region for the loads acting on the cross section.

In the context of principal equilibrium, this failure surface takes the form of a polygon, that is, a bidimensional surface obtained from the variation in the position of the neutral axis z, from line a to line b, covering all failure domains. These variations are specified by the designer and provided as input data for the solution. The smaller the increment in the variation of the neutral axis position, the smoother and more accurate the representation of the surface will be.

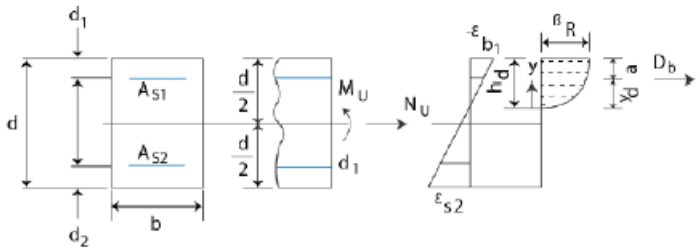


Figure 1. Section equilibrium

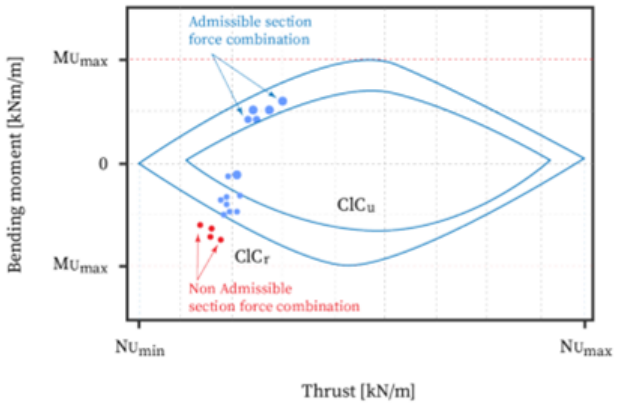


Figure 2. Failure surface

5 Pos processing application

A Python application was developed for the post-processing of results from numerical simulations using the finite element method with solid elements. The application reads the stress tensors at the nodes of the finite elements within a study cross-section and generates a response surface to facilitate the query and integration of stresses at any section of the model. For the interpolation, the Radial Basis Function (RBF) method, available in the Python library SciPy, was employed.

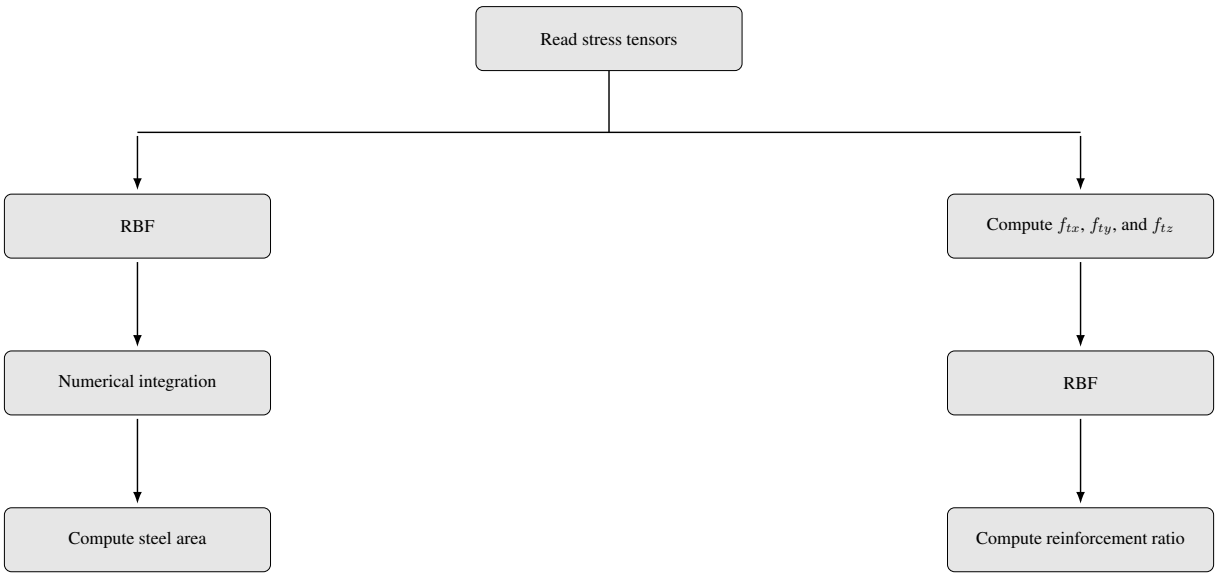


Figure 3. Flowchart: reading, RBF, integration, and steel/reinforcement calculations.

6 Case study

This section presents a case study of a wind turbine foundation modeled and analyzed in Plaxis 3D using ten-node quadratic tetrahedral solid elements. Similar to the structure, the soil was also modeled with solid elements. Compression-only interface elements were employed to represent the contact between the foundation base and the soil. The prestressed tie rods of the anchor cage were modeled using elements with tensile stiffness only. The loads were applied through a rigid plate. The geometries of the foundation and the anchor cage are shown in the Figure 4 below.

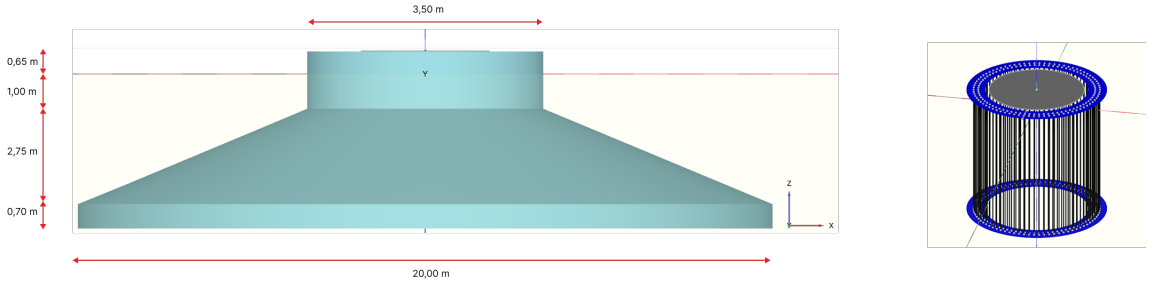


Figure 4. Geometries of the foundation and the anchor cage

The specific weight and modulus of elasticity adopted for the concrete were:

Table 2. Material parameters adopted in the analysis

Material	γ (kN/m^3)	E (MPa)	ν
Soil	18	100	0.3
Concrete	25	30 000	0.2
Steel	78	210 000	0.3

The adopted finite element mesh is shown in the Figure 5 below.

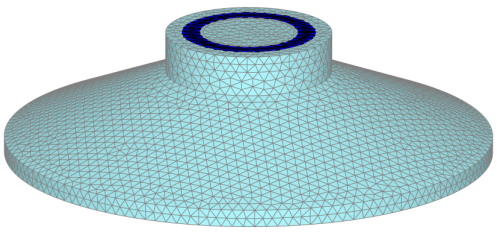


Figure 5. Finite element mesh

Table 3. Applied forces

	F_{xy} (kN)	F_z (kN)	M_{xy} (kN·m)	M_z (kN·m)
Value	1735	-7942	188.5×10^3	1632

6.1 Comparison of Internal Forces Between Solid and Shell Models

To enable a direct comparison between solid and shell elements, a shell-element model was developed with identical mechanical parameters and loading conditions to those of the solid model. The base skirt was discretized into concentric rings, each with a difference of 1.0 m between the outer and inner radii. The simulation results, along with the percentage differences between the two modeling approaches, are presented in the Figure 6 and table below.

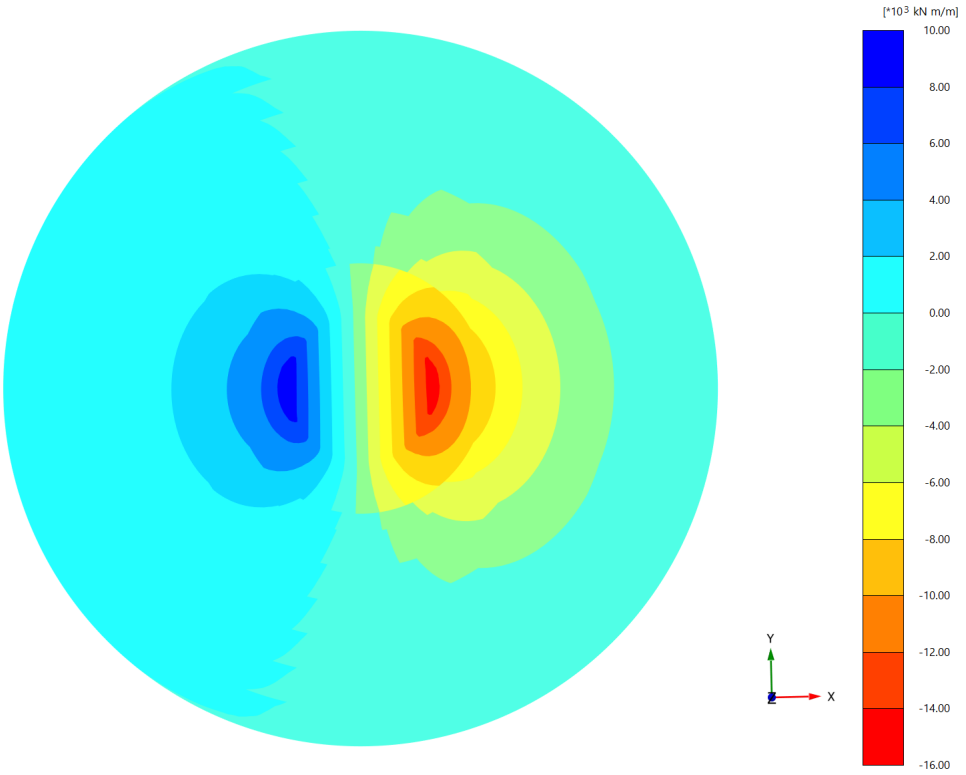


Figure 6. $M_{11}x$ design moments

Table 4. Applied forces

type	Md_{5m} (kN·m)	Md_{6m} (kN·m)	Md_{7m} (kN·m)	Md_{8m} (kN·m)	Md_{9m} (kN·m)
Solid	3457	3080	2586	2037	1235
Shell	4214	3389	2113	1615	753
Diff.%	$+22$	$+10$	-18	-21	-39

It can be observed that, for the adopted discretization and element formulation, even in regions of the foundation where the structural behavior exhibits a bending-dominated response, there is a considerable deviation in the results when compared to those obtained with solid elements.

The σ_x output generated by the developed application for a section in a vertical plane passing through the line $(0, 0)$–$(1, 0)$ is shown in the Figure 7 below.

The calculated internal forces and the corresponding failure envelope for a 35 MPa concrete are shown in the Figure 8 below.

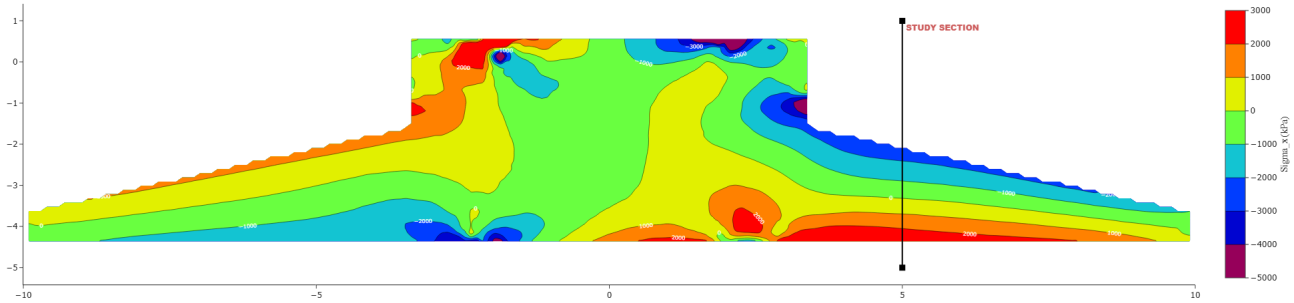


Figure 7. σ_x stress

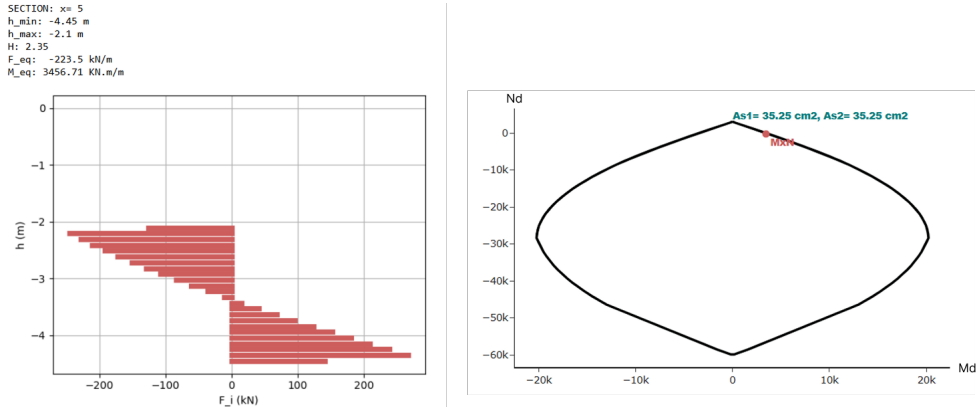


Figure 8. Internal forces at R=5m and failure surface

6.2 RSM results

The results obtained using the RSM method are presented in this section.

The variation of the reinforcement ratio estimated by the RSM method is shown in Figure 9 below. The equivalent reinforcement ratio obtained for the section at R = 5,m was 0.19%, which is 26% higher than that obtained from the principal equilibrium design, thus automatically confirming the premise of the ultimate limit state theory. However, it is noteworthy that this difference decreases for greater radii, and the method also enables the distribution of reinforcement in regions where the stress state is markedly three-dimensional, for which design based on combined bending is not applicable.

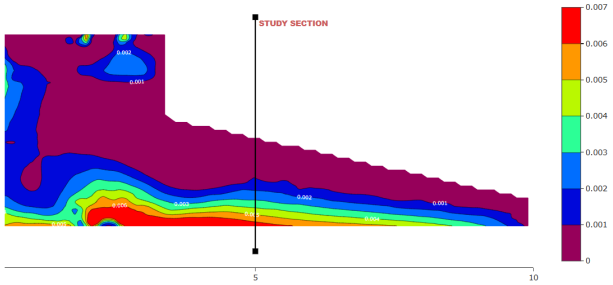


Figure 9. RSM reinforcement ratio distribution

Table 5. RSM reinforcement ratio

type	ρ_{5m}	ρ_{6m}	ρ_{7m}	ρ_{8m}	ρ_{9m}
RSM	0,19	0,175	0,16	0,15	0,12

7 Conclusions

This study presented a methodology for the structural analysis of reinforced concrete structures using solid finite elements. The results demonstrated that modeling with shell elements may lead to incompatible internal force values due to the inherent limitations of such elements in accurately representing the geometry and stress distribution in wind turbine foundations.

The results obtained through the Reinforced Solid Method (RSM) were consistent with those from the principal equilibrium approach and offered the additional advantage of enabling the reinforcement layout in the pedestal region, where the structural behavior differs from classical bending–compression or bending–tension conditions.

Finally, it is worth noting that extending the use of solid elements to the soil–structure interaction analysis of wind turbine foundations offers several additional advantages. In addition to the more representative behavior resulting from mesh continuity, the adoption of more realistic constitutive models enables coupled analyses of complex behaviors, such as the evaluation of rotational stiffness based on models that account for the degradation of the soil shear modulus.

For future developments, the proposed methodology could be extended to include the assessment of additional concrete failure criteria, as well as the verification of concrete compressive capacity based on the fundamental principles of the RSM, thereby broadening its applicability and enhancing its reliability for practical engineering design.

Acknowledgements. The authors would like to express their gratitude to Araxá Engenharia for encouraging the development of this work and supporting their participation in the event.

Authorship statement. The authors hereby confirm that they are the sole liable persons responsible for the authorship of this work, and that all material that has been herein included as part of the present paper is either the property (and authorship) of the authors, or has the permission of the owners to be included here.

References

[1] B. H. R. *Estudo de Fundação Direta de Aerogeradores com Métodos Numéricos*. UFSC, 2019.
[2] B. J. C. D. Bittencourt T. N.. Chen R. Design of reinforced concrete structures from three-dimensional stress fields. *IBRACON Structures and Materials Journal*, vol. 16, n. 4, 2023.
[3] K. Lundstedt. *IEC TC88 - 61400-6 Tower and Foundation design*. IEC, 2015.
[4] S. S. B. Problems of calculating the strength of massive concrete and reinforced concrete elements of complex hydraulic structures. *Power Technol. Eng.*, vol. 17, n. 9, pp. 471–476, 1983.
[5] I. I. Kamezawa N. Hayashi and T. M. A study on design methods of rc structures based on fem analysis. *Proc. Jpn. Soc. Civ. Eng.*, vol. 25, n. 502, pp. 103–122, 1994.
[6] M. N. Marti P. and F. S. J. Dimensioning of orthogonally reinforced concrete solids. *Struct. Concr. Switzerland, fib-CH, fib-Congr.*, vol. , pp. 18–23, 2002.
[7] M. P. Foster S. J. and M. N. Design of reinforcement concrete solids using stress analysis. *ACI Struct. J.*, vol. 100, pp. 758–764, 2003.
[8] N. M. P. and H. C. *Limit Analysis and Concrete Plasticity*. Boca Raton: CRC Press, 2011.
[9] A. M. A. *Dimensionamento de peças de concreto armado em python.* 1. ed. Curitiba: UFPR, 2024.